Novel Dopant Activation of Heavily Doped p^+-Si by High Current Densities

J. S. Huang and K. N. Tu

Department of Materials Science and Engineering, University of California at Los Angeles, Los Angeles, California 90095-1595
(Received 15 July 1996)

Novel dopant activation in the heavily boron-doped p^+-Si was created by applying an electrical current of high current density. The p^+-Si was implanted by 40 keV BF_2^+ of 5×10^{15} ions/cm^2 and annealed at 900 °C for 30 min to obtain a partial boron activation. For additional activation, we gradually applied current until a current density of 5×10^6 A/cm^2 was achieved. The resistance of the p^+-Si responded by gradually increasing, then decreasing with a precipitous drop. The resistance was reduced by a factor of 5 to 18. Mechanisms of the novel dopant activation are proposed.   [S0031-9007(96)01839-X]

Ion implantation has been widely used to dope Si for making shallow junction devices. Host lattice damage by ion implantation must be repaired to achieve dopant activation and to recover carrier mobility [1,2]. Postimplantation annealing, typically at 800–1000 °C for 30 min or rapid thermal annealing (RTA) at 1100 °C for 1 sec, is required [3,4]. However, for a heavily doped Si ($>10^{20}$ ions/cm^{-3}), these conventional annealings are incapable of achieving complete activation and have been an outstanding issue for some time [5–11]. Higher temperature annealing is undesirable, as it increases thermal budget and broadens the junction. In this Letter, we report a novel activation of B dopants in p^+-Si by applying a high current density ($>5 \times 10^6$ A/cm^2) at room temperature. We found that the resistance of the p^+-Si can be reduced by a factor of 5 to 18 over that of conventional annealing. We can activate the supersaturated B.

(100) Si wafers, 3–5 Ω cm, n-type, were oxidized to a thickness of 300 nm oxide. Photolithography and buffered HF etching were used to define Si channel regions within the oxide. A screen oxide was grown to 20 nm thick for filtering and capping the implanted ions. The wafers were implanted with a dosage 5×10^{15} ions/cm^2 of BF_2^+ accelerated to 40 keV. The projected range was 0.3 μm. Postimplantation annealing at 900 °C for 30 min in N_2 ambient was carried out to activate B dopants without the removal of the capping oxide. Sheet resistance of the p^+-Si channels was 85.7 $\Omega/\square$. To achieve further activation, electrical contacts were made. A 300 nm low temperature oxide was then grown on the p^+-Si. A set of square contact windows, $10 \times 10, 8 \times 8, 6 \times 6, 4 \times 4, 2 \times 2, 1 \times 1$ μm^2, were opened to the channel region by photolithography and buffered HF etching. Finally, metal films (Ni, Ti, or Al) of thickness 260 nm were deposited to make contacts to the p^+-Si. The metal bond pads were defined by photolithography with a lift-off process in acetone. Shown in Fig. 1 are the top and side views of the test structure. We prepared samples of the p^+-Si channels with different lengths (50, 70, 95, 97.5, 100, 140, and 175 μm) and widths (1, 2, 4, 6, 8, and 10 μm). The chan-

nel width was matched with the contact size and different Ohmic contacts (Ni/p^+-Si, Ti/p^+-Si, Ni/silicide/p^+-Si, and Al/p^+-Si) were used. The resistance changes of the p^+-Si channels together with the contacts at different applied currents, ranging from 1 to 80 mA, were measured using a Keithley current source and voltage meter. We also studied the resistance changes at different temperatures (25, 100, and 200 °C).

Figures 2(a) and 2(b), respectively, show the voltage drop across the p^+-Si (10 μm wide and 175 μm long) and the corresponding resistance change as a function of applied current at three different temperatures. It can be seen in Fig. 2(b) that the resistance increases gradually then reaches a maximum value at a "critical current," defined as the current at which the resistance is a maximum. Beyond that, the resistance decreases gradually. This electrical behavior which has the appearance of a resistance peak is temperature dependent, as shown by the three curves in Fig. 2(b). The critical current decreases with increasing temperature. The samples of Ni/p^+-Si, Ti/p^+-Si, Al/p^+-Si, and Ni/silicide/p^+-Si were studied. They all show the same electrical behavior, indicating that it is independent of the contacts and is merely due to the p^+-Si channel. We note that the
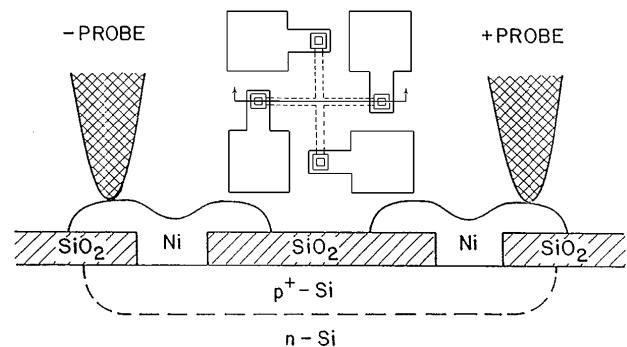

FIG. 1.   Schematic of the test structure (the inset in the middle shows the top view). A p^+-Si channel is shown. Current is applied to the Si channel, and the voltage drop across the channel is measured.
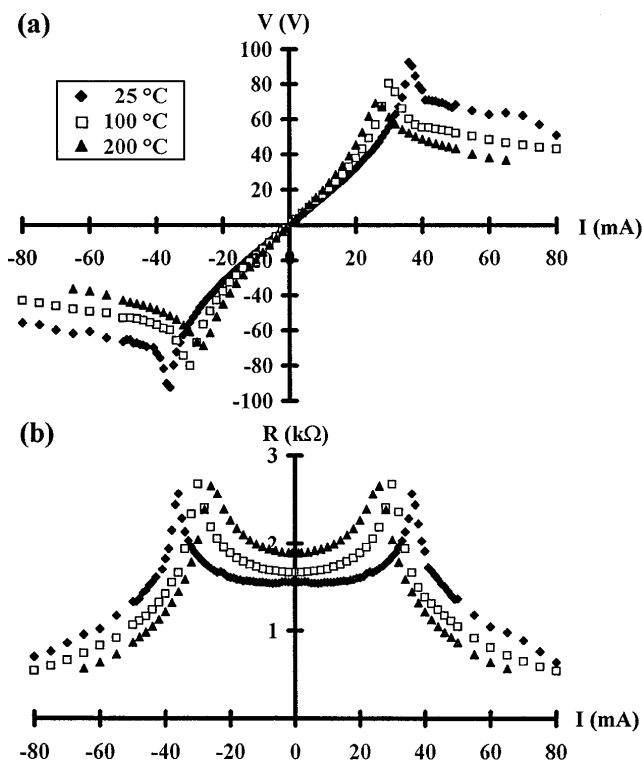
(a)

(b)

FIG. 2.   The electrical properties of the p^+-Si as a function of temperature. (a) A plot of voltage vs applied current. (b) A plot of resistance vs applied current at different temperatures (25, 100, and 200 °C). The critical current, where the resistance (or voltage) is maximum, decreases with increasing temperature.

resistance is in the $k\Omega$ range, which rules out the contribution of the contacts in the $1-10$ Ω range. The specific contact resistivity of the metal/p^+-Si contacts are about $(2-5) \times 10^{-6}$ Ω cm^2 measured by Kelvin bridge.

The resistance of the p^+-Si as a function of channel width was also investigated. Shown in Fig. 3 are the resistances of the samples with the same length (100 μm) but
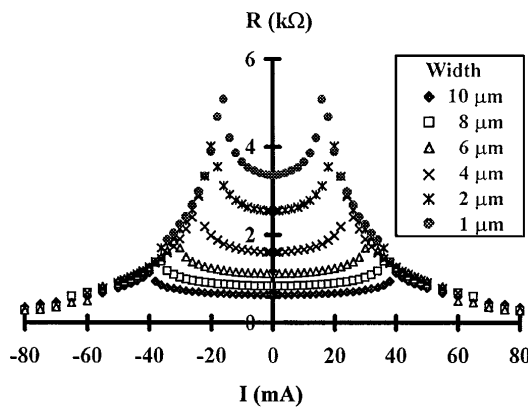

FIG. 3.   Resistance vs applied current for the p^+-Si at 25 °C. Samples with different channel widths were used. The critical current increases with increasing width.

different widths (10, 8, 6, 4, 2, and 1 μm) at room temperature. Several unique features were observed. First, the narrower the channel width, the higher the current density, and the faster the rise in resistance. While the 10 μm sample showed a wide Ohmic regime, the 1 μm sample showed a negligible one. Second, the critical current, where the resistance is maximum, increases with increasing width. Third, the magnitude of resistance increase, from the initial value to the maximum value, decreases with increasing width. Fourth, the graduate decrease of resistance after the critical current also decreases with increasing width.

We found that the electrical behavior shown in Fig. 2 is reversible as long as the current is below 80 mA. The rate of current increase and decrease used was about 0.5 mA/sec. Table I lists the critical current densities (J_{crit}) for the p^+-Si as a function of channel width "w." The critical current density is defined by the relationship: $J_{crit} = I_{crit}/(w \times t)$, where I_{crit} is the critical current and t is the depth of the p^+-Si channel and is estimated to be about 0.15 μm. For the p^+-Si, the critical current densities are in the range of $(2-6) \times 10^6$ A/cm^2, as listed in Table I. The critical current densities were found to be a function of temperature, as the critical currents shown in Fig. 2; they decrease with increasing temperature. The activation energy Q_{crit}, determined from a plot of J_{crit} vs $1/kT$, is a function of channel width. The activation energy varies from 0.55 eV for the 10 μm wide to 0.28 eV for the 1 μm wide, as shown in Table I.

A dramatic event occurred when the applied current was increased to about 80 mA. Figure 4 shows the resistances of the p^+-Si (10 μm wide and 100 μm long) for four consecutive runs as a function of applied current at room temperature. The resistance curve of the first run followed the upper curve and showed the same electrical behavior as shown in Figs. 2 and 3. However, the resistance dropped precipitously at 80 mA, corresponding to about a current density of 5×10^6 A/cm^2 (Fig. 4). Interestingly, the curves of the second and third runs followed the lower curve; no peak appeared as in the upper curve. The resistance decreased significantly (by a factor of 5) as comparison with the postimplantation annealing value.

The p^+-Si channels of different width were also studied. All showed a large resistance decrease by a factor of 5 to 18 upon a high applied current density, as indicated by the ratio of R_1/R_2 in Table II and plotted in Fig. 5. To test the stability of the channels after the resistance drop, we annealed the sample at 450 °C for 30 min. The fourth run indicated that it was stable and very little change was observed (see Fig. 4, and compare R_2 and R_3 in Table II). We found that, instead of ramping up the current, we could achieve the large resistance drop instantaneously by applying directly the "activation current," defined as the current where the abrupt resistance drop occurs. The "activation current density," $J_{activ}[= I_{activ}/(w \times t)]$, was found to increase with decreasing width.

TABLE I. The critical current densities (J_{crit}) and the activation energies (Q_{crit}) of the p^+-Si as a function of channel width (w) (samples No. 1 to No. 6) at 25 °C. The activation energies are determined from J_{crit} vs $1/kT$.

			p^+-Si			
Sample	No. 1	No. 2	No. 3	No. 4	No. 5	No. 6
l (μm)[a]	100	100	100	97.5	95	95
w (μm)[b]	10	8	6	4	2	1
J_{crit} (10^6 A/cm^2)	2.5	2.8	3.1	3.3	4.4	6.0
Q_{crit} (eV)	0.55	0.62	0.55	0.34	0.28	0.28

[a]The nominal length is 100 μm. Because of contact size, the length is slightly shorter for the narrowed channels with smaller contacts. We are studying the length to see if it has an effect on the critical current density.
[b]Narrow channels, especially the 1 and 2 μm, are not well defined due to lithography and etching.

The mechanisms for the electrical inactivity of boron in heavily doped Si are still controversial [12]. The mobile interstitial silicon atom produced during ion implantation damage [13] may have a strong influence on the formation of the excess boron. In the following section, we attempt to explain the observed resistance changes, especially the peak and drop, in terms of rearrangement of the implanted dopant atoms. For a highly doped p^+-Si, the dopant concentration may reach beyond the solubility limit set by the postimplantation annealing temperature. In this study, a dose of 5×10^{15} ions/cm^2 of $BF_2{}^+$ at 40 keV was implanted into Si. The average concentration was 3.3×10^{20} ions/cm^{-3} of B, which is obtained from dividing the dose by the projected range. At an annealing temperature of 900 °C, the solubility of boron was 5×10^{19} ions/cm^{-3} [5,6], which was much smaller than the average concentration of the implanted boron. Consequently, only part of the boron atoms were activated, leaving behind a large amount of excess boron to form SiB_x clusters [5,14].

We speculate that, under the stress of a high current density, the SiB_x clusters can be dissociated into B interstitials. The scattering of the interstitials raises the resistance.
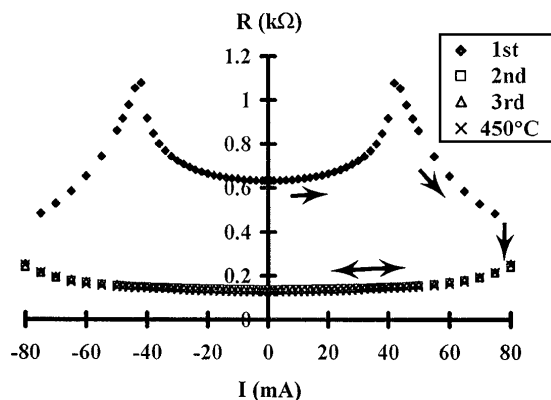

FIG. 4. Resistance vs applied current for the p^+-Si at four consecutive runs at 25 °C. The first run (incompletely activated) follows the upper curve. The second and third runs (nearly completely activated) follow the lower curves. The last run (after 450 °C 30 min annealing) followed the curves of the second and third runs. Ni/p^+-Si contacts were used.

As the applied current increases, an increasing number of boron atoms become interstitials. At the critical current, where the resistance is maximum, we suggest that the solubility of interstitial B has been reached. Beyond that, each B interstitial starts to couple with a lattice Si atom to form a B-Si split interstitial dumbbell pair; the resistance begins to decrease. This is the onset of dopant activation induced by a high current density.

We further speculate that, as the current further increases, more and more of the B-Si dumbbell pairs are formed. As a result, the resistance of the p^+-Si decreases gradually all the way to below the original value. The aforementioned electrical behavior of the p^+-Si is reversible; i.e., if we reduce the applied current, the dumbbells will part and clusters will reform.

At an extremely high current, defined as the activation current (80 mA in the case of the 10 μm wide line, as shown in Fig. 4), the resistance of the p^+-Si drops abruptly. This implies a nearly complete activation of boron dopants. The large resistance reduction is permanent. The resistance curve of the activated p^+-Si shows a stable behavior, as shown by the lower curve in Fig. 4. We speculate that at the precipitous drop, the B atom in the dumbbell pair displaces its Si mate into an interstitial site and becomes a substitutional dopant itself. The substitutional B dopants are quite stable, even beyond the solubility limit, at 450 °C for 30 min. Since activation can be achieved instantaneously by applying the activation current directly, no long range diffusion of B atoms, or Si atoms, is required in this mechanism.

In Fig. 2 we note that the resistance (below the critical current) increases with temperature. This is also true for the resistance of the activated p^+-Si (the lower curves in Fig. 4). We speculate that the metallic behavior may be due to the scattering from the clusters or interstitials which are responsible for the reduced carrier mobility. On the other hand, the large drop of resistance could also be influenced by carrier mobility. It is a subject to be studied.

We also note that the resistance (R_1 in Table II) is not proportional to the reciprocal of the cross-sectional area ($w \times t$) of the channel, especially for the 1 and 2 μm channels. The size effect can also be seen from the decrease in the activation energy (Q_{crit}) with the

TABLE II.   The resistance of the p^+-Si (100 μm long) of as-received (R_1), activated by current (R_2), and thermal annealed at 450 °C for 30 min (R_3) as a function of channel width (w).   The activation current densities (J_{activ}) are higher in narrower channels.

Sample width w (μm)	900 °C-30 min as-received R_1 (Ω)	Current activated R_2 (Ω)	450 °C-30 min annealed R_3 (Ω)	R_1/R_2	J_{activ} (10^6 A/cm^2)
10	633	132	125	5	4.8
8	818	116	102	7	6.3
6	1140	108	117	11	8.1
4	1600	94	88	17	11.3
2	2537	143	128	18	15.6
1	3355	192	171	18	18.3

decreasing channel width shown in Table I as well as the greater resistance drop with the narrower channels plotted in Fig. 5.   For all the size effects, it is plausible that the pattern formation and the lateral spread [15] from the mask edge in ion implantation might have influenced the narrower channels, hence the two-dimensional model of implantation and dopant activation should be examined for small structures.   Specifically, the effects of fluorine defects and strain in the channel edges, caused by the capped postimplantation annealing, may be important [16].   At the moment, we cannot explain the size effects in Tables I and II.   However, it is clear that this method of dopant activation by high current densities is more efficient for smaller size structures.

In conclusion, we have shown the activation of boron dopants in the p^+-Si by high current densities.   This new method of activation may activate dopants beyond their solubility limits as imposed by the conventional thermal annealing.   The activation current density needed is above 5×10^6 A/cm^2 for implanted B.   A large resistance reduc-

tion, by a factor of 5 to 18 over that of thermal annealing, has been achieved.   While much of the activation mechanism is uncertain and many process parameters have yet to be explored, this finding is nevertheless very exciting.
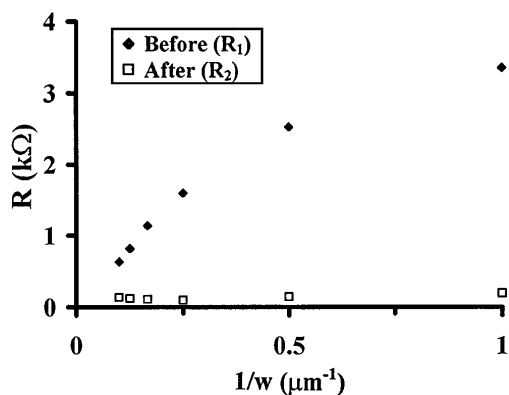
[1] H. Ryssel and I. Ruge, *Ion Implantation* (Wiley, New York, 1986).
[2] J. W. Mayer, L. Eriksson, and J. A. Davies, *Ion Implantation in Semiconductors* (Academic, New York, 1970).
[3] T. E. Seidel, D. J. Lischner, C. S. Pai, R. V. Knoell, D. M. Maher, and D. C. Jacobson, Nucl. Instrum. Methods Phys. Res., Sect. B **7/8**, 251 (1985).
[4] M. E. Lunnon, J. T. Chen, and J. E. Baker, J. Electrochem. Soc. **132**, 2473 (1985).
[5] H. Ryssel, K. Müller, K. Haberger, R. Henkelmann, and F. Jahnel, Appl. Phys. **22**, 35 (1980).
[6] F. N. Schwettmann, J. Appl. Phys. **45**, 1918 (1974).
[7] A. Armigliato, D. Nobili, P. Ostoja, M. Servidori, and S. Solmi, in *Semiconductor Silicon 1977,* edited by H. Hulff and E. Sirtl (Electrochemical Society, Princeton, 1977), p. 638.
[8] W. K. Hofker, H. W. Werner, D. P. Oosthoek, and N. J. Koeman, Appl. Phys. **4**, 125 (1974).
[9] L. J. Borucki, *International Electron Devices Meeting* (IEEE, San Francisco, 1990), p. 753.
[10] G. L. Vick and K. M. Whittle, J. Electrochem. Soc. **116**, 1142 (1969).
[11] J. Kato, J. Electrochem. Soc. **141**, 3158 (1994).
[12] P. M. Fahey, P. B. Griffin, and J. D. Plummer, Rev. Mod. Phys. **61**, 289 (1989).
[13] G. D. Watkins, Phys. Rev. B **12**, 5824 (1975).
[14] W. K. Hofker, H. W. Werner, D. P. Oosthoek, and H. A. M. de Grefte, Appl. Phys. **2**, 265 (1973).
[15] S. Furukawa, H. Matsumura, and H. Ishiwara, Jpn. J. Appl. Phys. **11**, 134 (1972).
[16] B. Holm and K. B. Nielsen, J. Appl. Phys. **79**, 1807 (1996).

FIG. 5.   The resistances of the p^+-Si (100 μm long) before and after the application of activation current density at 25 °C. Different channel widths (1−10 μm) are shown.